Existence of an operative pathway from the endoplasmic reticulum to the immature poxvirus membrane

Matloob Husain, Andrea S. Weisberg, and Bernard Moss†

Laboratory of Viral Diseases, National Institute of Allergy and Infectious Diseases, National Institutes of Health, Bethesda, MD 20892

Contributed by Bernard Moss, October 25, 2006 (sent for review October 3, 2006)

In thin sections of cells infected with vaccinia virus or other poxviruses, the viral membrane is first discerned as a crescent or circle lacking obvious continuity with a cellular organelle, presenting an appearance of *de novo* membrane biogenesis. This notion, which many consider heretical, is nevertheless consistent with the absence of a signature of endoplasmic reticulum (ER) trafficking, such as signal peptide cleavage or glycosylation, in any of the numerous viral membrane proteins. The purpose of this study was to determine whether an operative pathway exists between the ER and the immature virion membrane. We showed that the highly conserved A9 viral membrane protein was inserted into the ER of uninfected cells with the same topology as in viral membranes. Next, we found that replacement of the nonessential cytoplasmic tail of A9 with one containing COPII-binding sites reduced incorporation of the modified A9 into viral membranes and led to its accumulation in the Golgi apparatus, implying that A9 was inserted into the ER and then diverted from its natural path. Most importantly, we demonstrated cleavage of a heterologous signal peptide fused to the N-terminal region of A9 and localized the truncated protein in immature and mature virions. Additionally, immunoelectron micrographs showed A9 in tubules containing protein disulfide isomerase, an ER lumenal protein, near immature viral membranes. The present data provide strong evidence for an operative pathway from ER domains within the virus factory to the viral membrane.

membrane protein trafficking | vaccinia virus | virus assembly

The derivation of viral membranes from cellular membranes is a corollary of the axiom that all membranes arise from preexisting ones. Nevertheless, the origin of the initial lipoprotein membrane of vaccinia virus (VACV) and other poxviruses has perplexed investigators, even leading to suggestions that it may be synthesized *de novo*. The VACV membrane was first discerned in discrete cytoplasmic assembly regions as a crescent lacking obvious continuity with a cellular organelle (1–3), although tubular extensions were sometimes seen at the ends of the crescents (4–8). The crescent develops into a spherical immature virion (IV), which subsequently condenses into an infectious oval-shaped mature virion (MV) that contains exclusively nonglycosylated proteins. Some MVs are wrapped by trans-Golgi or endosomal cisternae containing additional viral proteins, most of which are glycosylated, providing the outer coat of the extracellular virion (EV) (9).

There have been considerable efforts to determine a cellular origin of the IV membrane. Immunoelectron microscopy of infected cells indicated the presence of viral transmembrane proteins in smooth tubules that react with antibodies to endoplasmic reticulum (ER) and ER–Golgi intermediate compartment (ERGIC) markers and the occurrence of such tubules near and possibly connected to viral crescent membranes (4, 7, 8, 10–12). However, the presence of viral proteins in the secretory pathway could represent escape from the correct route to the viral membrane. The latter idea is consistent with the finding of small amounts of glycosylated A14 protein in cytoplasmic extracts but not in virions (13). Moreover, ER, ERGIC, or Golgi proteins were not detected in the crescent membranes, and continuity between the latter and cytoplasmic tubules has been disputed (2, 3). Similarly controversial is the nature of the IV and MV membranes, specifically whether they are composed of one (1–3, 14) or two (8, 15, 16) sets of lipoprotein bilayers.

The use of pharmacological agents and dominant-negative inhibitors with known activities provides an alternative approach to investigate the formation of the viral membrane. Ulateo *et al.* (17) found that brefeldin A, which prevents binding of COPI coats to ERGIC and Golgi membranes, was without effect on IV and MV formation but prevented the subsequent wrapping of MVs to form EVs. That study confirmed the different origins of the IV and EV membrane, because only formation of the latter requires an intact Golgi compartment. Punjabi and Traktman (18) reported that the drug H89, a protein kinase inhibitor whose effects include interference with the assembly of COPII ER exit sites, prevented recovery of temperature-sensitive mutant virus replication after lowering the temperature, although neither IV formation nor protein trafficking was examined directly. In contrast, we reported that a dominant-negative Sar-1 GTPase, which specifically inhibits COPII transport from ER to Golgi membranes, had no effect on IV or MV production but did prevent wrapping of MVs and the subsequent formation of EVs (19). The latter study suggested that the IV membrane might arise from the ER itself, although this too remained unproven because none of the viral proteins incorporated into purified MVs have a signature of ER translocation, such as signal peptide cleavage or glycosylation. Moreover, the data could also be interpreted in terms of *de novo* origin of the IV membrane. A central question, therefore, is whether a functional pathway exists between the ER and the IV membrane.

Results

Similar Topology of A9 in ER and Viral Membranes. The VACV A9 protein, an integral component of the IV and MV membrane that is conserved in all poxviruses (20), was selected for the present analysis. Our first consideration was whether A9 would be incorporated into the ER of uninfected cells and, if so, whether the topology would be the same as in viral membranes. Another study (20) had shown that an influenza hemagglutinin (HA) epitope tag at the C terminus of A9 had no effect on A9 function, and this construct was therefore used here for detec-

Author contributions: M.H. and B.M. designed research; M.H. and A.S.W. performed research; M.H., A.S.W., and B.M. analyzed data; and M.H. and B.M. wrote the paper.

The authors declare no conflict of interest.

Freely available online through the PNAS open access option.

Abbreviations: ER, endoplasmic reticulum; ERGIC, ER–Golgi intermediate compartment; EV, extracellular virion; HA, hemagglutinin; IV, immature virion; MV, mature virion; PDI, protein disulfide isomerase; TM, transmembrane; VACV, vaccinia virus.

†To whom correspondence should be addressed at: National Institutes of Health, 4 Center Drive, Bethesda, MD 20892. E-mail: bmoss@nih.gov.

This article contains supporting information online at www.pnas.org/cgi/content/full/0609406103/DC1.

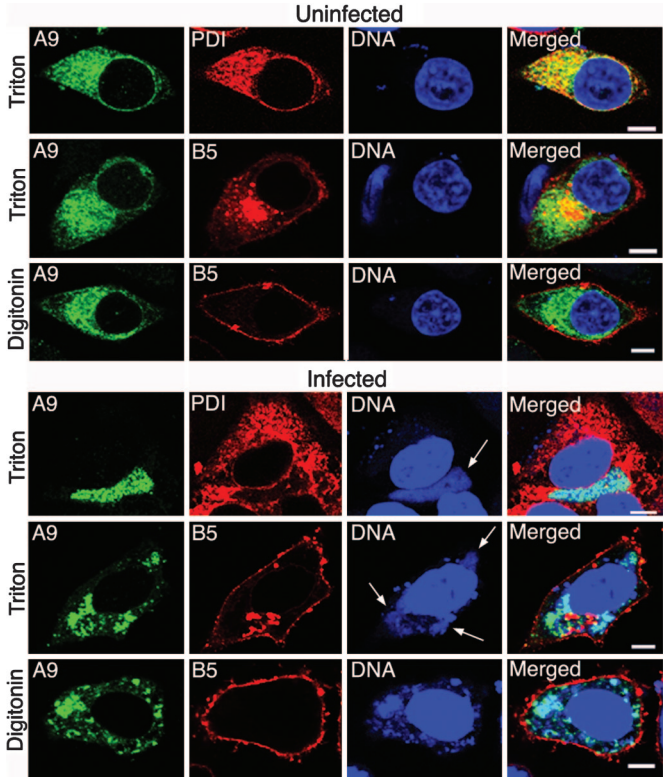

Fig. 1. Localization of A9 in uninfected and infected cells. Uninfected (*Upper*, rows 1–3) show the intracellular location of A9 in transfected HeLa cells. HeLa cells were transfected with a plasmid expressing A9 under the CMV promoter (row 1) or cotransfected with plasmids expressing A9 and B5 (rows 2 and 3). After 22 h, cells were fixed and permeabilized with Triton X-100 (rows 1 and 2) or digitonin (row 3). Cells were stained with rabbit anti-HA polyclonal antibody (row 1) or mouse anti-HA mAb (rows 2 and 3), followed by Alexa Fluor 488-conjugated anti-rabbit or anti-mouse IgG, respectively. Cells were then stained with mouse anti-PDI mAb (row 1) or rat anti-B5 mAb (rows 2 and 3), followed by Alexa Fluor 594-conjugated anti-mouse or Alexa Fluor 568-conjugated anti-rat IgG. Infected (*Lower*, rows 4–6 show the intracellular location of A9 in HeLa cells that were infected with vA9i in the absence of inducer and transfected with a plasmid expressing A9 under its natural promoter (rows 4–6). At 16 h after infection, cells were fixed, permeabilized with Triton X-100 (rows 4 and 5) or digitonin (row 6) and stained to detect A9, PDI, and B5 as above. Finally, cells were stained with DAPI and visualized by confocal microscopy. The rightmost column is a three-color merge. Green, Alexa Fluor 488; red, Alexa Fluor 568 or 594; blue, DAPI; (Scale bars, 10 μm.) Arrows indicate viral DNA factories.

tion of A9 by an HA mAb. HeLa cells were transfected with an A9-HA plasmid, and the distribution of the protein was determined by confocal microscopy after Triton X-100 permeabilization. A9 had a perinuclear and cytoplasmic reticular pattern that largely overlapped with the ER lumenal protein disulfide isomerase (PDI) (Fig. 1, row 1). The location of A9 was distinct from that of B5 (Fig. 1, row 2), a type I membrane protein component of the VACV EV that accumulates in the trans-Golgi complex and plasma membrane of uninfected cells (21, 22). The topology of A9 was determined by selectively permeabilizing the plasma membrane with digitonin (23). In digitonin-treated cells, A9 interacted with anti-HA mAb, indicating that the C-terminal epitope is accessible on the cytoplasmic side of the ER (Fig. 1, row 3). As a control for nonspecific permeabilization, the digitonin-treated cells were also stained with an antibody to the lumenal N-terminal domain of B5, which reacted with B5 on the cell surface but not within the ER or trans-Golgi apparatus (Fig. 1, row 3). Cotranslational association of A9 with microsomal membranes and the absence of a cleavable signal peptide were also demonstrated [see supporting information (SI) Fig. 5 and *Supporting Experimental Procedures*].

Localization of A9 in VACV-infected cells was facilitated by use of a conditional lethal mutant, vA9i, which encodes an inducible A9 protein (20). When synthesis of A9 is repressed, VACV IV membranes form, but subsequent steps in viral morphogenesis are blocked. In the present studies, cells were infected with vA9i in the absence of inducer so that untagged A9 expressed from the viral genome would not compete with HA-tagged A9 expressed from a transfected plasmid. In addition, the VACV A9 promoter was used, ensuring that transcription would take place only in appropriate cytoplasmic virus factories, where the viral RNA polymerase is located. The biological significance of the transfection was confirmed by demonstrating complementation of vA9i replication by the plasmid containing the HA-tagged A9 gene (SI Fig. 6 and *Supporting Experimental Procedures*). HA-tagged A9 was primarily associated with viral factories, which are recognized by DAPI staining of DNA (Fig. 1, row 4) and in IV membranes (shown later by immunoelectron microscopy). Note that DAPI-stained DNA factories may appear as a single discrete body or as numerous small ones close to the larger DAPI-stained nucleus. The pattern of PDI staining suggested that the density of ER is less in virus factories than in the surrounding cytoplasm (Fig. 1, row 4). As expected, B5, expressed from the viral genome, was mostly associated with the Golgi complex and plasma membrane rather than the virus factory (Fig. 1, row 5), consistent with previous data. Importantly, the C terminus of A9 faced the cytoplasm, as demonstrated by HA antibody staining of digitonin-treated cells (Fig. 1, row 6), as in uninfected cells (Fig. 1, row 3). The lumenal domain of B5 was detected only on the plasma membrane of digitonin-treated cells (Fig. 1, row 6), confirming the selectivity of the permeabilization procedure for infected cells. In addition, the C terminus of A9 was shown to be on the outside of the MV, which faces the cytoplasm before release (20). These data indicate a similar topology of A9 in ER membranes of uninfected cells and in membranes of viral factories and MVs, consistent with a relationship between ER and viral membranes.

A9 is Diverted to Golgi Membranes When Its Cytoplasmic Tail Is Replaced by the Corresponding Segment of the VSV G Protein. The A9 protein is 108-aa long with a putative transmembrane (TM) domain from amino acids 44–68 (Fig. 2, diagram). The C-terminal tail from amino acids 69–108 has poor sequence conservation among poxviruses and is not required for viral infectivity, as shown by complementation of virus infectivity by a C-terminal truncated protein (SI Fig. 6). Accordingly, A9 still localized in the virus factory in the absence of the C-terminal segment (Fig. 2, row 2) and was inserted into the IV and MV membrane (data not shown). On the other hand, COPII-binding sites in the cytoplasmic tail of the VSV G protein are necessary for efficient transit from the ER to the Golgi apparatus (24, 25). We predicted that if A9 normally traffics from the ER to the IV membrane, then replacing the cytoplasmic tail of A9 with the corresponding portion of VSV G (Fig. 2, diagram) might divert the fusion protein to the Golgi apparatus and possibly beyond. However, if A9 does not normally use an ER pathway, then the presence of COPII-binding sites would not have a diversionary effect. We observed that most of the chimeric A9 colocalized with antibody to the β COP Golgi membrane marker in infected cells with reduced amounts in the virus factory (Fig. 2, row 3), indicating diversion from viral membranes. Consistent with this scenario, the cytoplasmic tail of VSV G decreased the ability of A9 to complement the formation of infectious virus (SI Fig. 6). Golgi membrane localization of the chimeric protein also occurred in uninfected cells (Fig. 2, row 4). The dominant-negative Sar-1(T39N) GTPase inhibitor of the COPII ER exit pathway

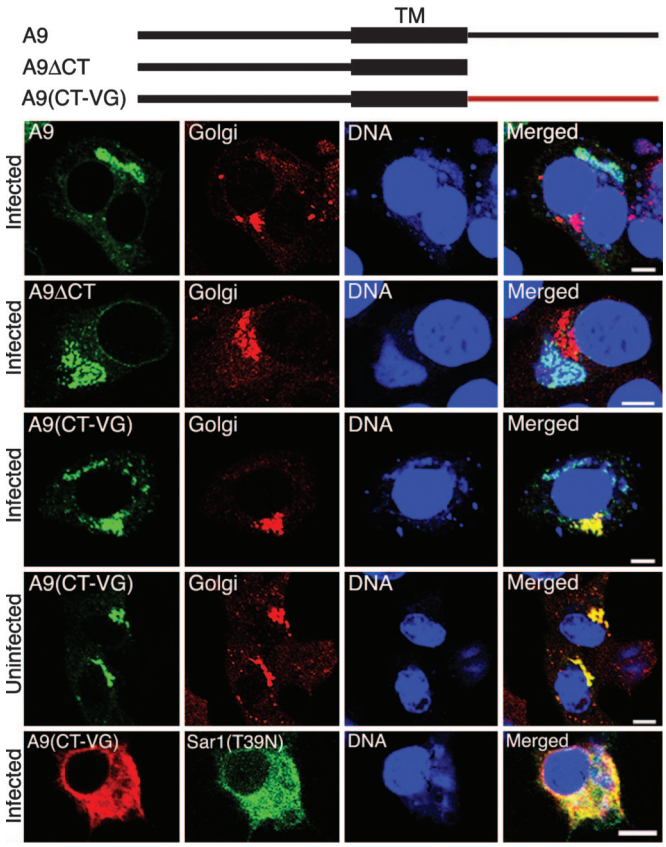

Fig. 2. Effect of the VSV G cytoplasmic tail on localization of A9. (*Upper*) Diagrams of A9, A9 without the cytoplasmic tail (A9ΔCT), and A9 with the VSVG cytoplasmic tail replacing that of A9 [A9(CT-VG)]. A9 sequences are in black, and VSVG sequences are in red. (*Lower*) Rows 1–3 show HeLa cells infected with vA9i and transfected with plasmids expressing full-length A9, A9ΔCT, or A9(CT-VG), regulated by the VACV A9 promoter. Row 4, uninfected HeLa cells transfected with a plasmid expressing A9(CT-VG) regulated by the CMV promoter. Row 5, HeLa cells cotransfected with a plasmid expressing A9(CT-VG) regulated by the A9 promoter and GFP-Sar-1(T39N) regulated by the CMV promoter; 24 h later, the transfected cells were infected with vA9i. At 16 h after infection (rows 1–3 and 5) or 24 h after transfection (row 4), cells were fixed, permeabilized, and stained with mouse anti-HA mAb, followed by Alexa Fluor 488-conjugated (rows 1–4) or Alexa Fluor 594-conjugated (row 5) anti-mouse IgG. Cells were then stained with rabbit anti-β COPI polyclonal antibody, followed by Rhodamine red-conjugated anti-rabbit IgG (rows 1–4). Finally, cells were stained with DAPI and visualized under a confocal microscope. Green, Alexa Fluor 488 or GFP (row 5, column 2); red, Rhodamine red, Alexa Fluor 594; blue, DAPI. (Scale bars, 10 μm.)

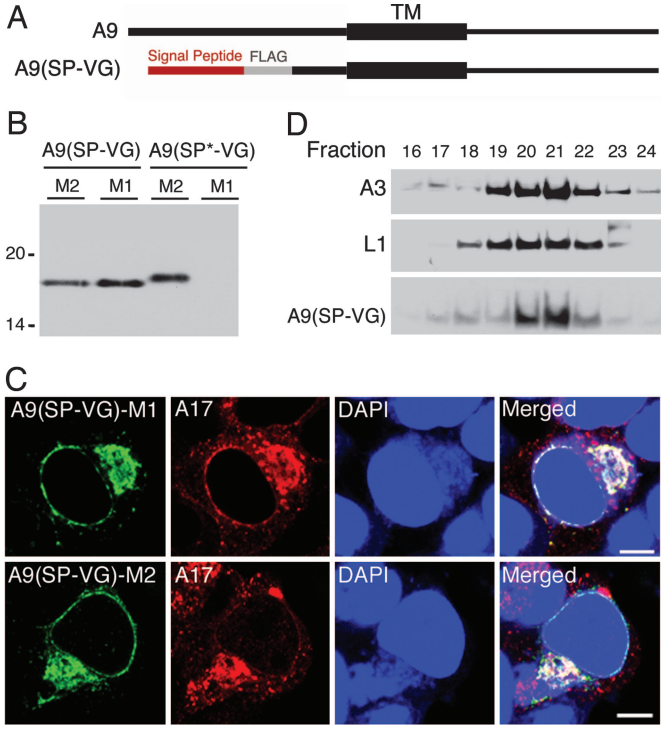

Fig. 3. Expression and localization of A9 derivative containing VSV G signal peptide in infected cells. (*A*) Diagrams of A9 and A9 with the cleavable signal peptide of VSV G replacing the N-terminal segment of A9 [A9(SP-VG)]. A9 sequences are in black, VSVG sequences are in red, and FLAG sequences are in gray. (*B*) HeLa cells were infected with vA9i and transfected with plasmids expressing A9(SP-VG) or a related plasmid with a noncleavable signal peptide [A9(SP*-VG)] regulated by the A9 promoter. At 16 h after infection, cells were harvested, and proteins were immunoprecipitated with anti-FLAG M1 or M2 mAbs. Polypeptides were resolved on 12% Bis-Tris polyacrylamide gel and transferred to a nitrocellulose membrane. The membrane was probed with the horseradish peroxidase-conjugated anti-HA antibody. (*C*) Localization of A9(SP-VG) in infected cells. HeLa cells were infected and transfected as in *A* and then fixed, permeabilized, and stained with mouse anti-FLAG M1 or M2 mAb, followed by Alexa Fluor 488-conjugated anti-mouse IgG. Cells were then stained with rabbit anti-A17 polyclonal antibody, followed by Rhodamine red-conjugated anti-rabbit IgG. Finally, cells were stained with DAPI and visualized by confocal microscopy. The rightmost column is a three-color merge. Green, Alexa Fluor 488; red, Rhodamine red; blue, DAPI. (Scale bars, 10 μm.) (*D*) Detection of signal peptide-cleaved derivative of A9 in purified MVs. HeLa cells were infected with VACV and transfected with a plasmid expressing A9(SP-VG). At 40 h after infection, cells were harvested, and virus was purified by a three-step procedure as described in *Experimental Procedures*. Fractions from the CsCl gradient were collected from the top of the tube, and proteins were resolved on 12% Bis-Tris polyacrylamide gel, transferred to a nitrocellulose membrane, and probed with mouse anti-FLAG M1 antibody, followed by horseradish peroxidase-conjugated anti-mouse antibody. The membrane was then stripped of antibodies and reprobed with rabbit anti-L1 and rabbit anti-A3 antibodies, followed by horseradish peroxidase-conjugated anti-rabbit antibody.

fused to GFP prevented localization of the chimeric A9 in the Golgi apparatus, confirming the usual route to the Golgi membranes in infected cells (Fig. 2, row 5). We also noted that blocking the ER exit of the chimeric A9 with Sar-1(T39N) did not appreciably enhance its localization in the virus factory.

Cleavage of a Signal Peptide Appended to the N Terminus of A9. As indicated earlier, none of the examined MV membrane proteins carry a signature of ER translocation such as signal peptide cleavage. This is also true for the A9 protein despite its N-terminal hydrophobicity; thus cleavage was not observed in an *in vitro* transcription/translation system with added dog pancreas microsomes (SI Fig. 5) or in transfected uninfected or infected cells (data not shown). We therefore decided to determine whether a heterologous signal peptide appended to A9 would be cleaved and whether the truncated protein would be incorporated into viral membranes. A chimeric *A9* gene, with DNA encoding the 34-aa N-terminal hydrophobic region of A9 replaced by DNA encoding the 16-aa signal peptide sequence of VSV G, followed by the 8-aa FLAG epitope tag (Fig. 3*A*), was inserted into a plasmid under the regulation of the natural A9 promoter to form pGA9(SP-VG). As a control, we constructed a second plasmid pA9(SP*-VG) identical to the first except for an inactivating amino acid substitution at the signal peptide cleavage site (26). The plasmids were transfected into cells infected with vA9i in the absence of inducer and A9 was analyzed by SDS/PAGE and Western blotting with two different mAbs to the FLAG epitope. Importantly, the M1 mAb is specific for an N-terminal FLAG epitope (27, 28) and therefore was predicted

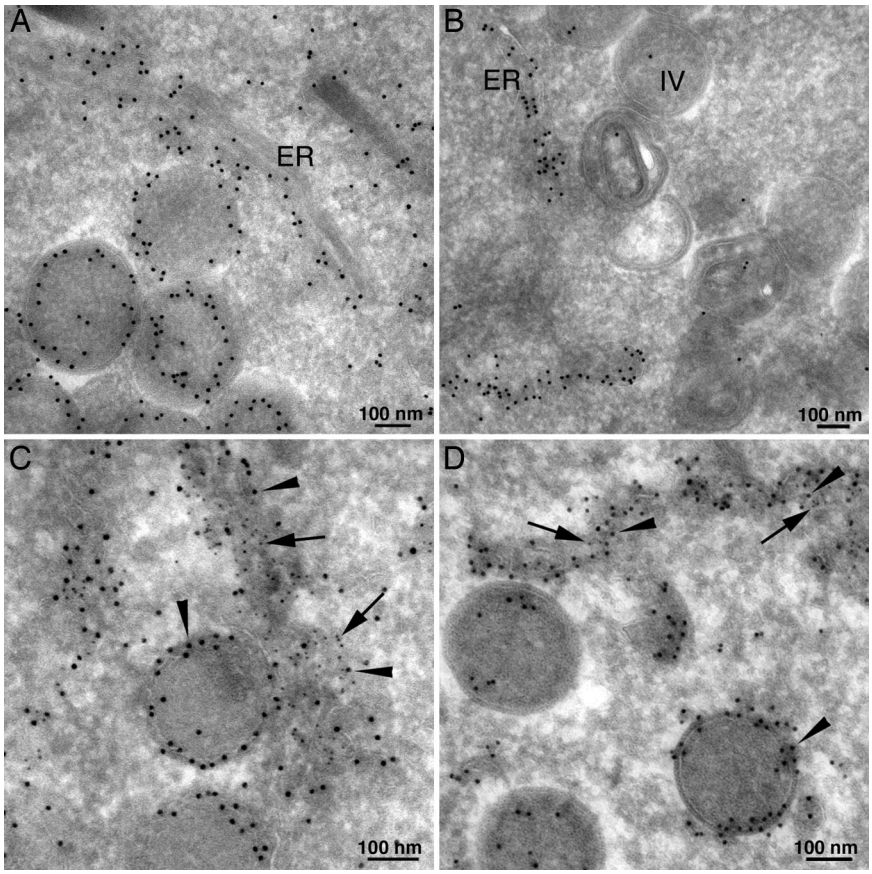

Fig. 4. ImmunoGold transmission electron microscopy. HeLa cells were infected with vA9i and transfected with plasmid pA9. (*A* and *B*) After 16 h, cells were fixed, cryosectioned, and stained with anti-HA mAb (*A*) or anti-PDI mAb (*B*), followed by rabbit anti-mouse IgG and protein A conjugated to 10-nm gold spheres. (*C*) Successive labeling with anti-HA (10-nm gold) and anti-PDI (5-nm gold). (*D*) Similar to *C*, except that the infected cells were transfected with pA9(SP-VG). Arrows and arrowheads point to 5- and 10-nm gold spheres, respectively. Bars indicate magnification.

to bind only to A9 that had been processed by signal peptidase. In contrast, the M2 mAb reacts with the FLAG epitope regardless of its position. As shown in Fig. 3*B*, the M1 and M2 mAbs reacted with the same size polypeptide in cells transfected with pGA9(SP-VG) indicating signal peptide cleavage. In contrast, the FLAG-tagged polypeptide expressed by pGA9(SP*-VG) had a slower mobility than the product of pGA9(SP-VG) and was recognized only by the M2 mAb, indicating absence of cleavage. We concluded that the signal peptide of the A9 protein expressed by pGA9(SP-VG) was specifically cleaved. The same two mAbs were then used to localize A9 containing a cleavable signal peptide by confocal microscopy. With both mAbs, there was fluorescent staining of the DNA factory region and a rim around the nucleus. The staining also largely coincided with the A17 IV membrane protein expressed from the viral genome, which is another marker of the virus factory (Fig. 3*C*).

The above data suggested that the signal peptide-cleaved A9 was inserted into the viral membrane. To prove this hypothesis, we needed to analyze purified MVs. However, N-terminal sequences of A9 that are important for maturation of MVs (M.H., unpublished results) had been deleted from pGA9(SP-VG). Therefore, we infected cells with wild-type VACV instead of vA9i and transfected them with pGA9(SP-VG). MVs were then purified by a rigorous multistep procedure including sedimentation through a sucrose cushion, rate zonal centrifugation in a sucrose gradient, and isopycnic centrifugation in CsCl. Each fraction of the CsCl gradient was then analyzed by SDS/PAGE and Western blotting with the M1 FLAG mAb to detect signal peptide cleaved A9(SP-VG) as well as antibodies to a core protein (A3) and another MV membrane protein (L1). As shown in Fig. 3*D*, all three antibodies reacted with correct-size proteins in the band of MVs. Thus, the presence of signal peptide-cleaved A9 protein in the MV provided conclusive evidence for transit between the ER and viral membrane.

Immunoelectron Microscopy of ER-Derived Tubules in Proximity to IVs. Experiments were carried out to localize A9 within virus factories. Cells were infected with vA9i in the absence of IPTG and transfected with a plasmid expressing wild-type A9 or pGA9(SP-VG) with HA epitope tags. Thin sections were stained with mAbs to HA and the ER lumenal PDI, followed by protein A coupled to 5- or 10-nm gold spheres. As shown in Fig. 4*A*, the mAb to HA decorated the perimeter of the IV as well as tubules near the IVs. (Note that the ring of labeling frequently appears to be inside the perimeter of the IV because of the thickness of the section and the exclusive labeling of the cut surface of the spherical particle as described (29). In Fig. 4*B*, the anti-PDI antibody labels ER with occasional gold grains close to IVs. Fig. 4*C* shows double labeling in which 10- and 5-nm gold grains were used to detect A9 and PDI, respectively. From such images, it was clear that A9 associated with both IV and ER-derived tubular membranes. The labeling of pA9(SP-VG)-transfected cells with the anti-HA mAb was similar showing the signal peptide-cleaved A9 in both IV and ER-derived tubules (Fig. 4*D*). The M1 antibody was not useful for immunoelectron microscopy because of unacceptable nonspecific staining of controls.

Discussion

Poxviruses are unusual in many respects: they replicate entirely in the cytoplasm and encode DNA replication and transcription enzymes as well as a redox system for cytoplasmic disulfide bond formation. Therefore, it would not be out of character for poxviruses to use novel mechanisms for membrane biogenesis. Indeed, the specialized site of poxvirus membrane assembly, the difficulty in proving continuity between the viral crescent membranes and cell organelles, and the absence of hallmarks of ER passage such as glycosylation or signal peptide cleavage in any MV protein point in that direction. Although some MV proteins were found associated with ER or ERGIC tubules in previous studies, this could have resulted from a minor amount of aberrant trafficking. Our task, therefore, was to determine the existence of an operative pathway between the ER and the IV membrane. The most unambiguous experimental result was demonstration of the cleavage of a heterologous signal peptide appended to the N terminus of the A9 protein and incorporation of this truncated protein into the MV membrane. The signal peptidase complex is anchored in the ER membrane so that the protease active site is intralumenal (30). Thus, cleavage of the heterologous signal peptide attached to A9 necessitated ER insertion. We assume that the signal peptide of the nascent chimeric protein interacted with the signal recognition particle to direct the ribosome to the ER where co-translational insertion occurred. The native A9 protein must be inserted in a similar way except the hydrophobic N terminus cannot be cleaved by signal peptidase.

A second informative experiment consisted of exchanging the nonessential C-terminal cytoplasmic segment of A9 with the corresponding domain of the VSV G protein, which interacts with the Sar-1 protein and the COPII complex. In this case, the chimeric A9 protein was largely diverted to the Golgi complex. The simplest interpretation is that after insertion of A9 into the ER membrane, the heterologous cytoplasmic tail misdirected the chimeric protein through the secretory pathway instead of allowing normal transit to the viral membrane. Misdirection could not have occurred unless the A9 protein had inserted into the ER. This result also suggested that IV proteins must lack COPII complex-binding sites, whereas such sites are likely to be present in viral proteins destined for the EV membrane, which is derived from modified trans-Golgi or endosomal membranes. Indeed, our previous studies showed that inhibition of COPII-mediated transport from ER exit sites by the dominant-negative SarI(H79G) protein does not prevent formation of IVs or MVs, although it does prevent trafficking of EV and other proteins to the Golgi apparatus and the wrapping of MVs. Similar results have been obtained with the dominant-negative SarI(T39G) protein (M.H., unpublished results).

It is interesting that truncation of either the N- or C-terminal segment of A9 did not prevent targeting to the IV membrane, suggesting the possibility of redundant signals or a signal in the transmembrane domain. A detailed analysis of the structural requirements for insertion of proteins into the IV membrane has been prepared (M.H., A.W., and B.M., unpublished work). Although the A9 protein may be representative of a class of viral proteins that transit to the IV membrane through the ER, other proteins may not. For example, the H3 protein has a C-terminal hydrophobic tail and *in vitro* experiments indicated association with microsomal membranes posttranslationally (31). Therefore, H3 and other viral proteins with a similar feature may insert directly into the IV membrane, although this process is yet to be demonstrated.

Confocal microscopy indicated less PDI staining in the virus factory compared with the surrounding cytoplasm, as previously observed (4). Similarly, there is less staining for the ERGIC 53 protein in the factory compared with the surrounding cytoplasm (19). Nevertheless, as we and others (4, 8) have shown, tubules and vesicles that stain with PDI as well as ERGIC markers are seen near crescent and IV membranes. The likely explanation for the low PDI staining is that the viral membranes form only a small part of the area of the factory. Importantly, the tubules near crescent and IV membranes were labeled with antibody to the A9 protein as well as PDI. We believe that the localization of A9 results from coordinated transcription and translation of viral mRNA, which is made in the factory (G. Katsafanas and B.M., unpublished work). Therefore, proteins incorporated into the ER residing outside of the factory might not be delivered to the IV membrane. We were unable to test this idea directly because of the dramatic shutdown of host cell protein synthesis at late times after infection. However, we have shown that the A9 protein synthesized in uninfected cells was not chased from the ER into IV membranes after infection (M.H., unpublished data).

For this study, we chose the A9 protein because it is not required for viral membrane assembly, thereby focusing the effects of protein modifications on trafficking. Consequently, the initial steps of viral membrane formation were not examined here. Previous studies had shown that several VACV proteins are needed to form recognizable viral membrane precursors; these include the F10 protein kinase (32) and the A11 (33), H5 (34), and G3 (35) proteins, none of which have TM domains. Repression of either the A17 (36, 37) or A14 (38, 39) membrane proteins leads to the accumulation of numerous vesicles and tubules. Determination of how each of these proteins contributes to viral membrane formation should make an intriguing story.

Experimental Procedures

Plasmids. Most expression plasmids were derived from pcDNA3 (Invitrogen, Carlsbad, CA) or pGEM7 (Promega, Madison, WI). Those used for transfection of uninfected cells, namely pHA-Sar-1(T39N) provided by J. Lippincott-Schwartz (National Institutes of Health), pGFP-Sar-1(T39N), pcA9, and pcA9(CT-VG) were regulated by the cytomegalovirus early promoter or the SV40 promoter in the case of pB5R (40). Plasmids transfected into infected cells, namely pGA9, pGA9ΔCT, pGA9(CT-VG), pGA9(SP-VG), and pGA9(SP*-VG) were regulated by the VACV A9L promoter.

Antibodies. Anti-HA.11 mouse mAb and rabbit polyclonal antibody that recognize the HA epitope were from Covance (Princeton, NJ). Anti-FLAG M1 and M2 mAbs were from Sigma–Aldrich (St. Louis, MO). Rabbit anti-A17LC polyclonal antibody, which recognizes the C-terminal peptide of the A17 protein, was described in ref. 37. Anti-B5 rat mAb 192C (41) was prepared from a hybridoma provided by J. Locker (European Molecular Biology Laboratory, Heidelberg, Germany). Rabbit anti-β COPI polyclonal antibody and mouse anti-PDI mAb were from BD Biosciences (San Jose, CA) and Stressgen Biolabs (Ann Arbor, MI), respectively. Alexa Fluor 488-conjugated anti-mouse IgG and anti-rabbit IgG, Alexa Fluor 594-conjugated anti-mouse IgG, Alexa Fluor 568-conjugated anti-rat IgG, and DNA-binding dye DAPI were from Molecular Probes (Eugene, OR). Rhodamine red-conjugated anti-rabbit IgG antibody was obtained from Jackson ImmunoResearch (West Grove, PA), and horseradish peroxidase-conjugated anti-HA antibody and anti-mouse and anti-rabbit antibodies were obtained from Roche (Indianapolis, IN) and ICN Biomedicals (Irvine, CA), respectively.

Transfection and Infection. The procedures were similar to those described in ref. 42.

Immunoprecipitation and Western Blotting. Procedures were essentially as described (19) except that 1 mM calcium chloride was included in buffers used with anti-FLAG M1 antibody.

Purification of MVs. MVs were isolated by mechanical disruption of VACV-infected HeLa cells, purified by sedimentation through a 36% sucrose cushion, and banded once on a 25–40% sucrose gradient as described (43). The virus was further purified on a 25–30% isopycnic cesium chloride gradient. Fractions were collected from the top, and proteins in each fraction were precipitated with trichloroacetic acid, resolved by SDS/PAGE, and analyzed by Western blotting.

Confocal and Transmission Electron Microscopy. Transmission electron and confocal microscopy was performed essentially as described (42).

We thank Robert Doms and Carolyn Machamer for critical reading of the manuscript and helpful suggestions.

1. Dales S, Mosbach EH (1968) *Virology* 35:564–583.
2. Heuser J (2005) *J Cell Biol* 169:269–283.
3. Hollinshead M, Vanderplasschen A, Smith GL, Vaux DJ (1999) *J Virol* 73:1503–1517.
4. Sodeik B, Doms RW, Ericsson M, Hiller G, Machamer CE, van't Hof W, van Meer G, Moss B, Griffiths G (1993) *J Cell Biol* 121:521–541.
5. Sodeik B, Griffiths G, Ericsson M, Moss B, Doms RW (1994) *J Virol* 68:1103–1114.
6. Ericsson M, Sodeik B, Locker JK, Griffiths G (1997) *Virology* 235:218–227.
7. Griffiths G, Roos N, Schleich S, Locker JK (2001) *J Virol* 75:11056–11070.
8. Risco C, Rodriguez JR, Lopez-Iglesias C, Carrascosa JL, Esteban M, Rodriguez D (2002) *J Virol* 76:1839–1855.
9. Smith GL, Vanderplasschen A, Law M (2002) *J Gen Virol* 83:2915–2931.
10. Sodeik B, Cudmore S, Ericsson M, Esteban M, Niles EG, Griffiths G (1995) *J Virol* 69:3560–3574.
11. Salmons T, Kuhn A, Wylie F, Schleich S, Rodriguez JR, Rodriguez D, Estban M, Griffiths G, Locker JK (1997) *J Virol* 71:7404–7420.
12. Krijnse-Locker J, Schleich S, Rodriguez D, Goud B, Snijder EJ, Griffiths G (1996) *J Biol Chem* 271:14950–14958.
13. Mercer J, Traktman P (2003) *J Virol* 77:8857–8871.
14. Grimley PM, Rosenblum EN, Mims SJ, Moss B (1970) *J Virol* 6:519–533.
15. Sodeik B, Krijnse-Locker J (2002) *Trends Microbiol* 10:15–24.
16. Griffiths G, Simons K, Warren G, Tokuyasu KT (1983) *Methods Enzymol* 96:466–485.
17. Ulaeto D, Grosenbach D, Hruby DE (1995) *J Gen Virol* 76:103–111.
18. Punjabi A, Traktman P (2005) *J Virol* 79:2171–2190.
19. Husain M, Moss B (2003) *J Virol* 77:11754–11766.
20. Yeh WW, Moss B, Wolffe EJ (2000) *J Virol* 74:9701–9711.
21. Ward BM, Moss B (2000) *J Virol* 74:3771–3780.
22. Lorenzo MM, Galindo I, Griffiths G, Blasco R (2000) *J Virol* 74:10535–10550.
23. Plutner H, Davidson HW, Saraste J, Balch WE (1992) *J Cell Biol* 119:1097–11116.
24. Nishimura N, Bannykh S, Slabough S, Matteson J, Altschuler Y, Hahn K, Balch WE (1999) *J Biol Chem* 274:15937–15946.
25. Sevier CS, Weisz OA, Davis M, Machamer CE (2000) *Mol Biol Cell* 11:13–22.
26. Shaw AS, Rottier PJ, Rose JK (1988) *Proc Natl Acad Sci USA* 85:7592–7596.
27. Prickett KS, Amberg DC, Hopp TP (1989) *BioTechniques* 7:580–589.
28. Stewart RS, Drisaldi B, Harris DA (2001) *Mol Biol Cell* 12:881–889.
29. Szajner P, Weisberg AS, Lebowitz J, Heuser J, Moss B (2005) *J Cell Biol* 170:971–981.
30. Shelness GS, Lin L, Nicchitta CV (1993) *J Biol Chem* 268:5201–5208.
31. da Fonseca FG, Weisberg A, Wolffe EJ, Moss B (2000) *J Virol* 74:7508–7517.
32. Traktman P, Caligiuri A, Jesty SA, Sankar U (1995) *J Virol* 69:6581–6587.
33. Resch W, Weisberg AS, Moss B (2005) *J Virol* 79:6598–6609.
34. DeMasi J, Traktman P (2000) *J Virol* 74:2393–2405.
35. Da Fonseca FG, Weisberg AS, Caeiro MF, Moss B (2004) *J Virol* 78:10238–10248.
36. Rodriguez JR, Risco C, Carrascosa JL, Esteban M, Rodriguez D (1997) *J Virol* 71:1821–1833.
37. Wolffe EJ, Moore DM, Peters PJ, Moss B (1996) *J Virol* 70:2797–2808.
38. Rodriguez JR, Risco C, Carrascosa JL, Esteban M, Rodriguez D (1998) *J Virol* 72:1287–1296.
39. Traktman P, Liu K, DeMasi J, Rollins R, Jesty S, Unger B (2000) *J Virol* 74:3682–3695.
40. Katz E, Wolffe EJ, Moss B (1997) *J Virol* 71:3178–3187.
41. Schmelz M, Sodeik B, Ericsson M, Wolffe EJ, Shida H, Hiller G, Griffiths G (1994) *J Virol* 68:130–147.
42. Husain M, Weisberg A, Moss B (2003) *Virology* 308:233–242.
43. Earl PL, Moss B (1998) in *Current Protocols in Molecular Biology*, eds Ausubel FM, Brent R, Kingston RE, Moore DD, Seidman JG, Smith JA, Struhl K (Greene Publishing Associates & Wiley Interscience, New York), Vol 2, pp 16.18.1–16.18.11.